



Research article

Tumour volume comparison between 16-row multi-detector computed tomography and 320-row area-detector computed tomography in patients with small lung tumours treated with stereotactic body radiotherapy: Effect of respiratory motion



Yusuke Iizuka^{a,*}, Mitsuhiro Nakamura^a, Satoshi Kozawa^b, Takamasa Mitsuyoshi^a, Yukinori Matsuo^a, Takashi Mizowaki^a

^a Department of Radiation Oncology and Image-applied Therapy, Graduate School of Medicine, Kyoto University, Kyoto, Japan

^b Division of Clinical Radiology Service, Kyoto University Hospital, Kyoto, Japan

ARTICLE INFO

Keywords:

Stereotactic body radiotherapy
Oncology
Computed tomography
Multi-detector CT

ABSTRACT

Purpose: We compared image quality and volume of a moving simulated tumour and of lung tumours in patients who were treated with stereotactic body radiotherapy (SBRT) in a 16-row multi-detector CT (MDCT) versus a 320-row area-detector CT (ADCT). Tumour volumes in each respiratory phase were also evaluated.

Materials and Methods: We acquired static and four-dimensional CT (4DCT) images of a moving phantom with 10- and 30-mm amplitudes with three periods of patterns (2, 4, and 6 s). Breath-hold and 4DCT images were acquired for 12 lung tumour patients who underwent SBRT. Image data were acquired via MDCT and ADCT. The tumours were delineated in each respiratory phase and their volumes in end-expiratory/end-inspiratory phase and mid-respiratory phase were compared.

Results: In the phantom study, tumour volumes were smaller and closer to the static image when evaluated by ADCT than by MDCT. In the clinical study, average tumour volumes \pm standard deviations were 9.58 ± 1.07 cm³ with MDCT (2.5-mm slice), and 7.12 ± 0.23 cm³ with ADCT ($p < 0.01$). Tumour volumes were closer to that of the breath hold CT in all patients evaluated by ADCT than by MDCT. Unlike MDCT, tumour volumes acquired by ADCT were smaller in end-expiratory or end-inspiratory phase than in the mid-respiratory phase.

Conclusions: Tumour volumes in each of the respiratory phases in ADCT were significantly smaller and closer to the static image than the corresponding volumes in MDCT. This suggests that treated volume can be reduced if ADCT is used in treatment planning.

1. Introduction

Stereotactic body radiation therapy (SBRT) for lung tumour has shown an excellent local control rate and has been recognized as a standard therapy for patients with inoperable lung tumours [1,2]. SBRT is also used to treat oligometastatic lung disease [3,4]. In lung SBRT, appropriate motion management is recommended, since target doses are affected by motion, mainly due to respiration. The American Association of Physicists in Medicine, Task Group 76, proposed five methods for controlling motion: motion-encompassing, respiratory-gating, breath-hold, forced shallow breathing with abdominal

compression, and real-time tumour-tracking (RTTT) [5]. Among these, respiratory-gating and RTTT methods have been used during respiratory-synchronized irradiation.

Use of any of these five techniques requires evaluation of respiratory motion accurately. To evaluate respiratory motion or target volume, four-dimensional CT (4DCT), in which respiratory signals are evaluated with the motion of the chest and/or abdominal wall or respiratory volumes, is widely used. It is important to acquire the accurate phase images in treatment planning of respiratory-synchronized irradiation with 4DCT, because a specific phase image is used as a reference, such as end-respiratory phase or mid-respiratory phase. There is no

Abbreviations: ADCT, area-detector, CT; CC, Crania-caudal; RTTT, real-time tumor-tracking; 4DCT, Four-dimensional CT; MDCT, Multi-detector CT; NSCLC, Non-small cell lung cancer; SBRT, Stereotactic body radiotherapy

* Corresponding author at: Department of Radiation Oncology and Image-applied Therapy, Graduate School of Medicine, Kyoto University, 54 Shogoin Kawaharacho, Sakyo-ku, KYOTO 606-8507, Japan.

E-mail address: yiizuka@kuhp.kyoto-u.ac.jp (Y. Iizuka).

<https://doi.org/10.1016/j.ejrad.2019.06.002>

Received 1 January 2019; Received in revised form 18 May 2019; Accepted 7 June 2019

0720-048X/© 2019 Elsevier B.V. All rights reserved.

consensus regarding which phase should be used in treatment planning with 4DCT. In our institution, we typically acquire 4DCT images with a 16-row multi-detector CT (MDCT) scanner to evaluate respiratory motion [6], but the reference image acquired by 4DCT with a MDCT scanner exhibits several problems, such as motion artefacts, which are severe in the mid-respiratory period, and misalignment artefacts, which often occur at the boundary of imaging range between the different couch positions. If the respiration pattern is not reproducible, artefacts often occur and the motion cannot be evaluated accurately [7]. Wide-detector CT, such as 320-row area-detector CT (ADCT), can acquire the entire trajectory of the tumour without couch movement. Thus, we can evaluate the movement of the tumour with this CT modality, which has been widely used in the cardiac field, and is used to evaluate the respiratory motion of lung tumours or breast cancers in research studies [8–11]. However, there is no study comparing MDCT and ADCT directly and there are no ADCT model designed for radiotherapy planning currently.

In this study, we compared the image quality and tumour volume acquired with MDCT and ADCT in a phantom and in patients with lung tumours who were treated with SBRT. We hypothesized that images would have less artefacts and tumour volumes would be more accurate when evaluated by ADCT than when evaluated by MDCT. We also evaluated the tumour volume between the end-respiratory and mid-respiratory phases.

2. Materials and methods

The clinical portion of this study was approved by our institutional review board; we obtained informed consent from all enrolled patients.

2.1. CT acquisition: ADCT

We used a 320-row ADCT scanner (Aquilion ONE, Canon Medical Systems, Otawara, Tochigi, Japan) to scan the patient's tumour and the phantom, using the same setting as described in a previous study [8]. Images were acquired in the continuous-volume mode (16 cm craniocaudal [CC] coverage per rotation). The time for a single rotation was 0.5 s. The collimation was 320 x 0.5 mm and reconstruction slice thickness was 1.0 mm. The scan settings were 120 kV and 50 mA. The respiratory signals were obtained using a respiratory gating system with a pressure sensor (AZ-733 V; Anzai Medical Co., LTD, Shinagawa, Tokyo, Japan). The pressure sensor was inserted into the belt which was fastened to the patient's abdomen and the respiratory signal was perceived as the cyclic change of the pressure. The image was acquired in one respiratory cycle, and an acquired image was sorted into 10 respiratory phase bins. The system calculated a respiratory phase, where 0% corresponded to the inhalation peak and 50% to the midpoint between consecutive inhalation peaks. Static images were also acquired as benchmarks in the phantom study.

2.2. CT acquisition: MDCT

A 16-row MDCT scanner (LightSpeed RT, General Electric Healthcare, Milwaukee, WI, USA) was also used to scan the tumour and the phantom. The time for a single rotation was 0.7 s. We used slice thickness and image reconstruction slice thickness of 1.25 and 2.5 mm in the clinical study because we used this setting in practice, while we evaluated not only the clinical setting but also a thinner setting (0.625 and 0.625 mm) to reduce bias due to differences in spatial resolution between ADCT and MDCT in the phantom study. The cine duration time of the scan at each couch position was > 6.0–8.0 s, which was greater than the maximum observed respiratory period in all patients. The scan settings were 120 kV and 100 mA. We acquired the whole trajectory of the simulated tumour in the phantom study and the tumour in the clinical study with conventional scanning. Simultaneously, the respiratory phase was monitored using the Varian Real-time Position

Management (RPM) system with an infra-red marker position (Varian Medical Systems, Inc., Palo Alto, CA, USA). The RPM system calculated a phase at each point of a respiratory tract, same as the ADCT, and CT slices were sorted into 10 respiratory phase bins with the Advantage SIM workstation (General Electric Healthcare). Static (Phantom Study) and end-expiratory breath-hold (Clinical Study) images were also acquired as benchmarks for the following phantom study and clinical study.

2.3. Phantom study

We acquired the static and 4DCT images of a moving phantom with MDCT and ADCT, following the above-mentioned protocol. The 4DCT images of a QUASAR phantom included a 30-mm diameter spherical object (a simulated tumour) and sinusoidal movement of approximately 10 and 30 mm in amplitude along the longitudinal axis in three cycle patterns (2, 4, and 6 s). The image of the experimental material on the ADCT is shown in Figure A.1. CT images were acquired three times in each setting to reduce artefacts associated with the measurement method and the average value was defined as the tumour volume.

2.4. Clinical study

Ten patients with early stage non-small cell lung cancer (NSCLC) or metastatic lung tumours, who were planned to undergo RTTT SBRT, were enrolled in this study. The patients were laid in the supine position with their arms up and were asked to breathe freely (not tidal or deep breath) during assessment by both systems. We did not use contrast enhance agent with both MDCT and ADCT acquisitions. The median interval between the MDCT and ADCT was 6 days (range, 1–11 days).

All images were transferred to the MIM maestro ver. 6.6 (MIM software Inc, Cleveland, OH, USA). The simulated tumour in the moving phantom in each phase was delineated automatically based on the Hounsfield Unit (HU) threshold, which indicated a known simulated tumour volume (14.1 cm³) of the tumour in the static CT image acquired with MDCT (-255 HU) and ADCT (-270 HU); region-growing segmentation, which expands the volume until a separate region appears around the tumour, was also used because we could not delineate the moving simulated tumour accurately with the HU threshold method. The lung tumours in patients in each phase were delineated automatically based on the region grow method. Then, their peripheral uncertainty due to the tumour's spicules, blood vessels, or chest wall next to the tumour's rim was modified by the radiation oncologists who were expert in SBRT.

The actual simulated tumour volume in the phantom study and the lung tumour volume in the end-expiratory breath hold CT acquired with MDCT (2.5 mm slice) in the clinical study were recognized as the benchmark. The average volumes and standard deviation of the simulated tumour and patient tumour in each respiratory phase were evaluated by ADCT and by MDCT, and then compared. Further, the average volumes of the tumour between the end-respiratory (0% and 50%) and mid-respiratory (30% and 70%) phases were also compared with the average target volumes of all respiratory phases. Tumour motion was measured as the maximum distance of the centre of the tumours among the phases. All statistical analyses were performed using R software [12]. The average tumour sizes were evaluated with Wilcoxon signed-rank test in each tumour and determined as statistically significant when the p value was < 0.05.

3. Results

3.1. Phantom study

The CT images in each phase were clearer on ADCT than on MDCT qualitatively. Using the HU threshold method, the tumour could not be delineated accurately on MDCT, mainly because of motion artefacts.

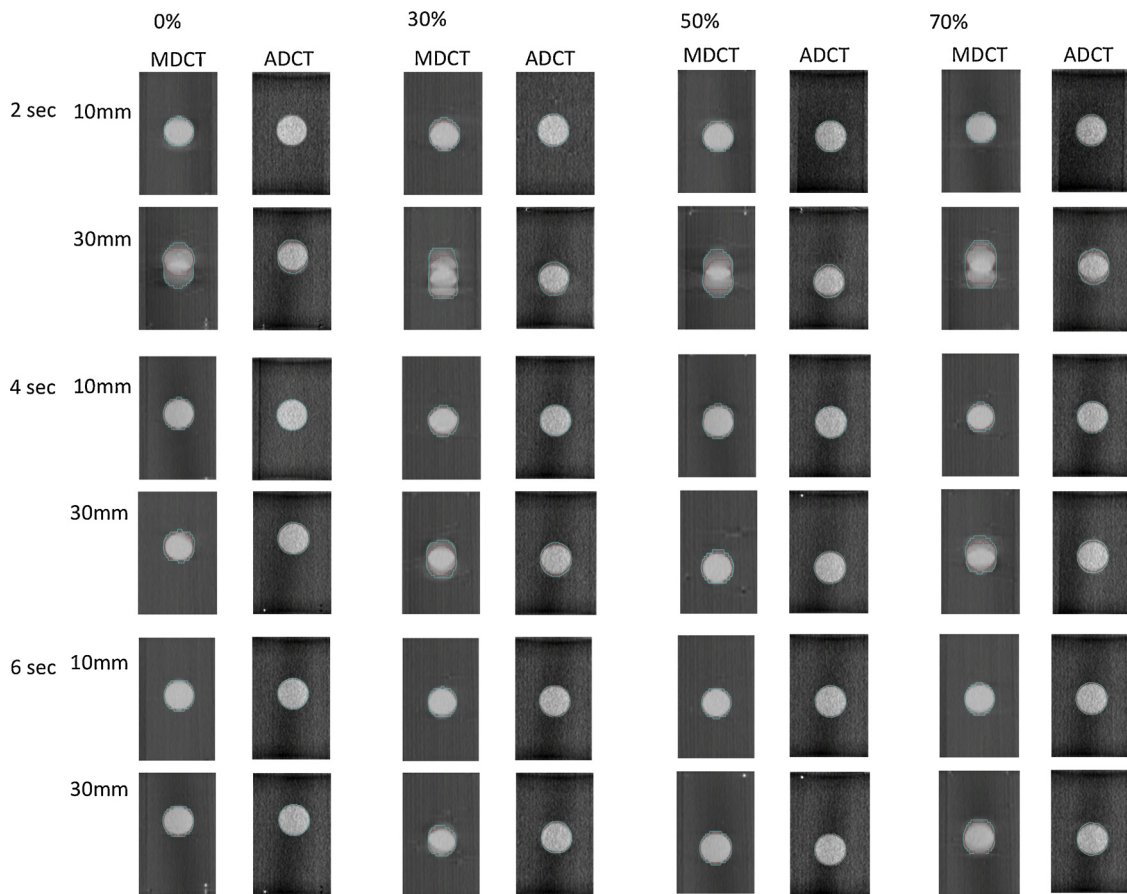


Fig. 1. Images of representative phases in the phantom study. The red lines indicate the tumour volume delineated by the CT value threshold method; the cyan lines indicate the volume delineated by the region grow method.

Abbreviations: MDCT = 16-row multi-detector CT, ADCT = 320-row area-detector CT

Table 1

Target volume (cm³) in the phantom study using the Hounsfield Unit threshold method and region grow method. The volume of the simulated tumour was 14.1 cm³. Average volumes ± standard deviations and the difference compared to the simulated tumour volumes are shown. p-values were calculated using Wilcoxon signed-rank test between ADCT vs MDCT with 2.5 mm slice thickness and ADCT vs MDCT with 0.625 mm slice thickness. Abbreviations: MDCT = 16-row multi-detector CT, ADCT = 320-row area-detector CT.

		Hounsfield Unit threshold			
Cycle	Motion	ADCT	MDCT(2.5 mm)	MDCT(0.625 mm)	p-value ADCT vs MDCT (2.5/0.625 mm)
2 s	10 mm	14.04 ± 0.06 (-0.4%)	13.99 ± 0.27 (-0.8%)	13.85 ± 0.43 (-1.7%)	0.85 / 0.23
	30 mm	13.77 ± 0.18 (-2.3%)	13.30 ± 1.49 (-5.7%)	12.50 ± 3.31 (-11.4%)	0.80 / 0.43
4 s	10 mm	14.08 ± 0.02 (-0.1%)	14.03 ± 0.37 (-0.9%)	13.94 ± 0.16 (-4.1%)	0.70 / 0.01
	30 mm	13.97 ± 0.08 (-0.9%)	13.62 ± 0.42 (-3.4%)	13.52 ± 0.74 (-4.1%)	0.02 / 0.10
6 s	10 mm	14.10 ± 0.01 (-0.0%)	14.18 ± 0.11 (0.63%)	15.50 ± 0.35 (9.8%)	0.04 / 0.02
	30 mm	14.26 ± 0.06 (1.2%)	14.01 ± 0.27 (-0.6%)	15.58 ± 0.66 (10.5%)	0.02 / 0.02

		Region grow			
Cycle	Motion	ADCT	MDCT(2.5 mm)	MDCT(0.625 mm)	p-value ADCT vs MDCT (2.5 / 0.625 mm)
2 s	10 mm	14.65 ± 0.14 (3.9%)	16.68 ± 0.56 (18.4%)	17.35 ± 0.88 (23.0%)	< 0.01 / < 0.01
	30 mm	16.89 ± 1.10 (19.8%)	22.64 ± 2.00 (60.6%)	21.85 ± 3.42 (55.0%)	< 0.01 / < 0.01
4 s	10 mm	14.72 ± 0.11 (4.4%)	15.84 ± 0.28 (12.3%)	15.46 ± 0.53 (9.7%)	< 0.01 / < 0.01
	30 mm	15.40 ± 0.36 (9.2%)	18.29 ± 1.22 (29.7%)	18.46 ± 1.14 (30.9%)	< 0.01 / < 0.01
6 s	10 mm	14.64 ± 0.22 (3.8%)	15.58 ± 0.35 (10.5%)	15.71 ± 0.43 (11.4%)	< 0.01 / < 0.01
	30 mm	15.01 ± 0.24 (6.4%)	16.71 ± 0.54 (18.5%)	17.37 ± 1.52 (23.2%)	< 0.01 / < 0.01

Imaged phase in the representative phase and each corresponding pattern are shown in Fig. 1. Videos of the simulated tumour are in the following links. Videos of MDCT were acquired with a slice thickness of 2.5 mm. (V1:MDCT 2sec-10 mm, V2:MDCT 2sec-30 mm, V3:MDCT 4sec-10 mm, V4:MDCT 4sec-30 mm, V5:MDCT 6sec-10 mm, V6:MDCT 6sec-30 mm, V7:ADCT 2sec-10 mm, V8:ADCT 2sec-30 mm, V9:ADCT

4sec-10 mm, V10:ADCT 4sec-30 mm, V11:ADCT 6sec-10 mm, and V12:ADCT 6sec-30 mm). The results of simulated tumour volumes are summarized in Table 1. The actual simulated tumour volume and evaluated with static state was 14.1 cm³. When using the HU threshold method, the simulated tumour volumes were evaluated slightly smaller in all patterns, except in 6-sec periods and 10-mm motion, when

Table 2

Patient and tumour characteristics. Abbreviations: M = male, F = female, Rt = right, Lt = left, S = lung segment, MDCT = 16-row multi-detector CT, ADCT = 320-row area-detector CT.

Patient #	Age(years)	Sex	Tumour diameter (mm)	Tumour Location	Days between MDCT and ADCT
1	85	M	13	Rt S6	11
2	74	M	40	Rt S6	9
3	85	F	15	Rt S9	12
4	80	F	15	Rt S10	5
5	88	M	20	Lt S10	4
6	76	M	30	Rt S6	5
7	84	M	35	Lt S5	4
8	74	M	32	Lt S6	1
9	73	F	37	Rt S10	7
10	78	M	28	Rt S10	6
11	77	M	20	Rt S6	6
12	64	M	10	Rt S6	4

acquired by MDCT than by ADCT. The evaluated tumour volumes were not always close to the that of in the static image. However, the tumour delineation was not accurate due to the artefacts which made the HU of the tumour decreased when using the HU threshold method. When using the region grow method, tumour volumes were significantly smaller and closer to the static image in all cases when evaluated by ADCT than by MDCT. Standard deviation of the tumour volume was clearly smaller in all cases when acquired with ADCT than with MDCT. Larger amplitude and faster moving cycle were associated with a lesser degree of distinction of the simulated tumour. The tumour volume differences between the reconstruction slice thickness of MDCT (2.5 mm vs 0.625 mm) were not significant.

3.2. Clinical study

In the clinical study, 12 patients (male, $n = 9$; female, $n = 3$) with early stage NSCLC or metastatic lung tumours, were enrolled between January 2013 and February 2014 and all CT images were successfully acquired. The mean age was 79 years (range, 64–88 years). Patient and tumour characteristics are summarized in Table 2.

The median tumour diameter was 24 mm (range, 10–40 mm); the median tumour motion was 11.5 mm (range, 5.0–38 mm) and 15.9 mm (range, 3.5–32.1 mm) on ADCT and MDCT, respectively. The median period of an averaged respiratory cycle was 4.8 s (range, 3.8–6.5 s) and 4.4 s (range, 3.0–9.8 s) on ADCT and MDCT, respectively. All the images were successfully acquired in regular respiration.

The images of the tumour in a representative patient are shown in Fig. 2. The images acquired with ADCT were clearer than those acquired with MDCT. There was a misalignment artefact at the tumour and the diaphragm on MDCT. Videos of the tumour can be found in the following links (V13: MDCT and V14: ADCT). The volume of the tumour in each phase was varied. The results are shown in Table 3. Average tumour volumes \pm standard deviations were $9.58 \pm 1.07 \text{ cm}^3$ with MDCT (2.5-mm slice), and $7.12 \pm 0.23 \text{ cm}^3$ with ADCT ($p < 0.01$). The tumour volumes were significantly smaller in all patients when evaluated by ADCT than by MDCT and the volumes were closer to that of the breath hold CT which were acquired by MDCT (2.5-mm slice) in all patients evaluated by ADCT than by MDCT. The average difference of the tumour volume was 29.7%. There was no correlation between the tumour volume difference and the tumour motion ($r = 0.20$) or respiratory period ($r = 0.02$).

Tumour size comparison among the respiratory phases is shown in Table 4. The average ratio of the differences of tumour volume in 0%, 30%, 50%, and 70% phases to the average tumour volume was less than 3% when evaluated by ADCT, and less than 10% when evaluated by MDCT. Comparison between the 0% and 50% phases, and the 30% and 70% phases, revealed a statistically significant difference in the average

tumour size on ADCT ($p < 0.001$), but there was no significant difference on MDCT ($p = 0.99$).

4. Discussion

In this study, we compared the images of a simulated tumour in a moving phantom and lung tumours in clinical cases, both of which were acquired using MDCT and ADCT. The image in each phase was clear and the tumour volume was small and close to the static images when using ADCT. Indeed, there are few reports regarding 4D motion evaluation of respiratory motion in other organs with wide-detector CT. For example, Yamashita et al. reported on the detection of metal clips or surgical staples in gastric or oesophageal cancer [10,11] and Mori et al. evaluated the motion of lung tumours with ADCT [9]. However, there is no report comparing the images and tumour volumes acquired with MDCT and ADCT directly.

In the phantom study, the volumes of simulated tumours, delineated with the region grow method and evaluated with ADCT, were smaller and closer to the static image than with MDCT. Though the difference of the method affected the results in the simulated tumour, we elected to use the region growing method because this method was reliable in the baseline phase images. The difference in the CT axial slice thickness in MDCT did not affect the results of the comparison of MDCT with ADCT. In the clinical study, the volumes of lung tumours were smaller and closer to the static image when evaluated with ADCT than when evaluated with MDCT. Our results indicate that the tumour volume was overestimated with MDCT during clinical cases and that we can reduce target volume by using ADCT during treatment planning. Although the tumour volume differences were relatively small and the benefit was slight in lung tumours, if we use ADCT for abdominal region such as the liver and pancreas, ADCT would provide an advantage by acquiring a clear image and reducing the target size. Tumour motion affected the image quality. Nakamura et al. reported that the velocity of the tumour affected its estimated size with MDCT; faster moving tumours were estimated to be larger [13]. Similarly, in the phantom study, we found that larger motions and shorter respiratory cycles were associated with more artefacts. We were able to acquire 4DCT images close to static images with less artefacts with ADCT mainly because we could acquire the images of moving tumours without couch shift. The difference of the spatial resolution might affect the artefacts of the images, the influence was limited based on the comparison of the reconstruction slice thickness in MDCT. In the clinical study, since the tumour motion and respiratory period were not constant, the correlation was not clear. The tumour motion is also affected with tumour location. The tumour located in lower lobe tend to move largely with respiration, and the tumour located near the heart is affected by heartbeat [14]. However, in this study, the relation was not clear between the tumour volume variation and the tumour location and between the tumour volume variation and the tumour motion. Thus, tumours evaluated in this study were located in the lower lung. We performed DTT-SBRT for the patients whose tumour moves more than 10 mm, then the tendency occurred. The tumour volume in each phase is important when a respiratory-synchronized method, such as respiratory gating and RTTT, is used. Onimaru et al. reported on the use of the end of the expiratory phase image to deliver respiratory gating radiotherapy with a real-time tumour-tracking system [15]. In gating radiotherapy, use of an end-expiratory phase is appropriate because the reproductively is high. However, there is no consensus regarding which phase should be used in delineating the target with 4DCT: end-respiratory phase or mid-respiratory phase during RTTT. Matsuo et al. reported that each phase in 4DCT was transferred to the expiratory breath-hold CT, based on the position of internal fiducial markers in lung tumours during RTTT [6]. Depuydt et al. reported on the use of end-expiratory phase in 4DCT to perform RTTT radiotherapy for lung and liver tumours within the same system [16]. In the present study, tumours in the mid-respiratory phase were significantly larger than those in the end-respiratory phase when

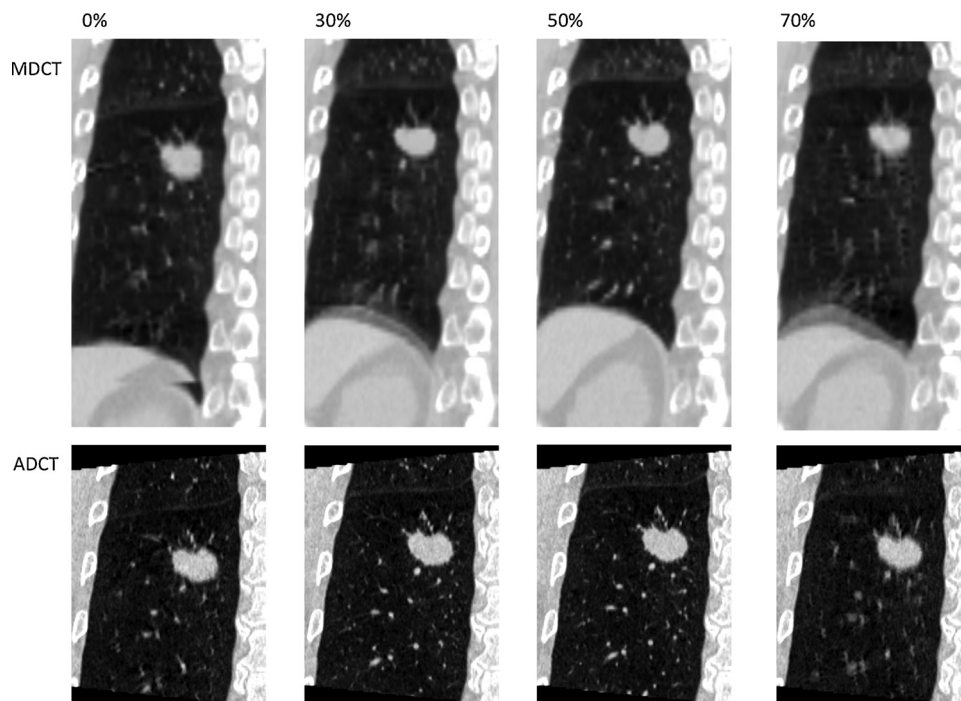


Fig. 2. Phase images of the tumour in a representative patient. Abbreviations: MDCT = 16-row multi-detector CT, ADCT = 320-row area-detector CT

evaluated by ADCT. The difference was caused by the motion artefact because the tumour motion was larger in the mid-respiratory phase than the end-inspiratory/end-respiratory phase [13]. However, the averaged difference was < 5% and there was no statistically significant difference in MDCT; thus, we suspect that the clinical impact was trivial. Of course, we should keep in mind that there were phases that demonstrated large differences to the mean volumes, such as the 0% phase in patient 10. Indeed, if a motion-encompassing method is used with or without abdominal compression, clinicians who use average image created from 4DCT phase images are not required to evaluate the tumour volume in each respiratory phase. However, they must generally delineate a larger volume, including the trajectory of the tumour motion, than required during the respiratory-synchronized method such as respiratory-gating or RTTT method. If the breath-hold method is used, the tumour image is clear and not distorted by artefacts due to respiratory motion; however, this method requires the addition of a margin to compensate for the error in every respiratory cycle [17,18]. In the scanning time, ADCT could be acquired in a few seconds over

several respiratory cycles. In contrast, MDCT requires multiple minutes to acquire a sufficient number of images to evaluate tumour motion, which can be utilized in a treatment plan. Regarding image quality, ADCT exhibits great advantages, relative to MDCT.

There are several limitations to this study. First, no commercial ADCT designed for radiotherapy treatment planning is currently available; thus, this result is not immediately applicable in clinical cases under the same conditions. The patient position in each CT method was not the same because we cannot use immobilization and laser positioning during ADCT scanning as we would during radiation therapy. The whole lung images could not be acquired with 4D ADCT. However, we could resolve this problem if ADCT were being used for a treatment plan, as image registration could be performed for separately acquired images such as 4DCT for evaluating the tumour motion and delineating the tumour, and whole lung CT for calculating the lung dose. Second, we could not acquire both CT images in the same day. Since the patient’s condition changed day to day, the tumour motion and respiratory period were varied in the same patients, as reported by Dhont

Table 3

Tumour volume in patient study. Average tumour volumes ± standard deviations are shown. “BHCT” indicates the tumour volume evaluated with MDCT (2.5-mm slice) in breath-hold. “Difference” indicates that the rate of the difference of tumour volume evaluated with ADCT compared to that of evaluated with MDCT. Abbreviations: BHCT = breath-hold CT, MDCT = 16-row multi-detector CT (2.5-mm slice), ADCT = 320-row area-detector CT.

Patient #	Tumour volume (cm ³)			Difference (%)	Tumour motion (mm)		Respiratory period (s)	
	BHCT	ADCT	MDCT		ADCT	MDCT	ADCT	MDCT
1	1.8	1.9 ± 0.1	2.7 ± 0.6	−31.3	31.0	24.4	5.0	5.6
2	22.1	23.1 ± 0.7	31.9 ± 2.70	−27.4	5.0	11.7	3.8	3.1
3	3.2	3.2 ± 0.2	3.7 ± 0.7	−22.4	33.2	27.5	4.2	4.8
4	3.9	4.0 ± 0.3	5.4 ± 1.1	−33.3	38.0	32.1	6.5	5.0
5	3.0	3.0 ± 0.1	4.5 ± 0.5	−35.1	8.8	5.3	4.1	3.0
6	17.6	17.3 ± 0.4	20.2 ± 1.7	−14.4	29.3	21.6	5.8	3.1
7	6.3	6.3 ± 0.2	7.5 ± 0.8	−18.1	5.5	3.5	4.5	3.5
8	8.9	8.4 ± 0.3	11.4 ± 1.0	−27.0	7.7	19.0	6.2	9.9
9	8.7	9.3 ± 0.3	13.1 ± 1.2	−28.8	11.8	12.9	6.1	4.4
10	3.3	3.2 ± 0.1	4.8 ± 1.2	−33.9	25.5	27.2	8.4	6.3
11	6.3	6.4 ± 0.2	8.9 ± 1.3	−27.3	11.2	11.4	3.8	3.1
12	0.5	0.5 ± 0.0	1.0 ± 0.2	−57.1	8.1	4.4	3.7	4.4

Table 4

Tumour volume rates in the end-inhale phase (0%), midpoint between the inhale peak phase (50%) and mid-respiratory phases (30% and 70%), compared with the average target volumes of all respiratory phases in the clinical study. Abbreviations: MDCT = 16-row multi-detector CT, ADCT = 320-row area-detector CT.

Patient #	0%		30%		50%		70%	
	ADCT	MDCT	ADCT	MDCT	ADCT	MDCT	ADCT	MDCT
1	0.94	0.72	1.09	0.88	1.03	0.86	1.02	1.11
2	0.95	1.13	1.00	0.99	1.00	1.03	1.05	0.97
3	0.99	0.84	1.00	0.87	0.99	0.85	1.01	1.31
4	0.97	0.86	1.02	0.85	0.94	0.89	1.04	0.96
5	1.02	1.04	1.03	0.91	0.96	0.91	1.05	1.00
6	0.99	0.96	1.03	0.95	1.01	0.90	1.01	1.04
7	1.04	0.87	1.04	0.84	0.99	1.07	0.98	1.04
8	1.05	0.96	1.03	1.03	1.00	1.02	0.98	0.91
9	0.95	1.00	1.01	1.03	0.99	0.98	1.02	0.89
10	1.01	1.50	1.05	0.85	0.98	0.79	0.99	0.74
11	0.95	1.00	1.01	0.89	0.98	0.92	0.99	0.97
12	0.87	1.14	0.97	0.79	0.94	0.77	1.09	1.16

et al. [19] and these differences might affect the results. Third, strictly speaking, the specifications and settings of each CT system were not same and the comparison might not fair. However, we decided that comparing the CT specification and setting itself were not useful and instead, we evaluated each CT system in the clinical setting. Lastly, the tumour volumes might have not been defined accurately. We used auto segmentation method to evaluate the tumour volume objectively, but we couldn't eliminate all variations or problems in auto segmentation.

The tumour volume in 4DCT was more accurately depicted when acquired with ADCT than with MDCT. Further investigation and development are required to use ADCT during treatment planning.

Transparency document

The [Transparency document](#) associated with this article can be found in the online version.

Appendix A. Supplementary data

Supplementary material related to this article can be found, in the online version, at doi:<https://doi.org/10.1016/j.ejrad.2019.06.002>.

References

[1] Y. Nagata, M. Hiraoka, T. Shibata, et al., A phase II trial of stereotactic body

radiation therapy for operable T1N0M0 non-small cell lung Cancer: japan clinical oncology group (JCOG0403), *Int. J. Radiat. Oncol. Biol. Phys.* 78 (3) (2010) S27–S28.

[2] R. Timmerman, R. Paulus, J. Galvin, et al., Stereotactic body radiation therapy for inoperable early stage lung cancer, *JAMA* 303 (11) (2010) 1070–1076.

[3] P. Okunieff, A.L. Petersen, A. Philip, et al., Stereotactic body radiation therapy (SBRT) for lung metastases, *Acta Oncol.* 45 (7) (2006) 808–817.

[4] K.E. Rusthoven, B.D. Kavanagh, S.H. Burri, et al., Multi-institutional phase I/II trial of stereotactic body radiation therapy for lung metastases, *J. Clin. Oncol.* 27 (10) (2008) 1579–1584.

[5] P.J. Keall, G.S. Mageras, J.M. Balter, et al., The management of respiratory motion in radiation oncology report of AAPM Task Group 76, *Med. Phys.* 33 (10) (2006) 3874–3900.

[6] Y. Matsuo, N. Ueki, K. Takayama, et al., Evaluation of dynamic tumour tracking radiotherapy with real-time monitoring for lung tumours using a gimbal mounted linac, *Radiother. Oncol.* 112 (3) (2014) 360–364.

[7] T. Yamamoto, U. Langner, B.W. Loo Jr, J. Shen, P.J. Keall, Retrospective analysis of artifacts in four-dimensional CT images of 50 abdominal and thoracic radiotherapy patients, *Int. J. Radiat. Oncol. Biol. Phys.* 72 (4) (2008) 1250–1258.

[8] Y. Iizuka, Y. Matsuo, S. Kozawa, et al., Optimization of a newly defined target volume in fiducial marker-based dynamic tumor-tracking radiotherapy, *Phys. Imag. Radiat Oncol.* 4 (2017) 1–5.

[9] S. Mori, M. Endo, S. Komatsu, T. Yashiro, S. Kandatsu, M. Baba, Four-dimensional measurement of lung tumor displacement using 256-multi-slice CT-scanner, *Lung Cancer* 56 (1) (2007) 59–67.

[10] H. Yamashita, S. Kida, A. Sakumi, et al., Four-dimensional measurement of the displacement of internal fiducial markers during 320-multislice computed tomography scanning of thoracic esophageal cancer, *Int J Radiat Oncol Biol Phy* 79 (2) (2011) 588–595.

[11] H. Yamashita, K. Okuma, W. Takahashi, et al., Four-dimensional measurement of the displacement of metal clips or postoperative surgical staples during 320-multislice computed tomography scanning of gastric cancer, *Radiat. Oncol.* 7 (2012) 137.

[12] Rd C.R. Team, A language and environment for statistical computing, R Foundation for Statistical Computing (2012).

[13] M. Nakamura, Y. Narita, A. Sawada, et al., Impact of motion velocity on four-dimensional target volumes: a phantom study, *Med. phys.* 36 (5) (2009) 1610–1617.

[14] Y. Seppenwoolde, H. Shirato, K. Kitamura, et al., Precise and real-time measurement of 3D tumor motion in lung due to breathing and heartbeat, measured during radiotherapy, *Int J Radiat Oncol Biol Phys* 53 (4) (2002) 822–834.

[15] R. Onimaru, M. Fujino, K. Yamazaki, et al., Steep dose-response relationship for stage I non-small-cell lung cancer using hypofractionated high-dose irradiation by real-time tumor-tracking radiotherapy, *Int. J. Radiat. Oncol. Biol. Phys.* 70 (2) (2008) 374–381.

[16] T. Depuydt, K. Poels, D. Verellen, et al., Treating patients with real-time tumor tracking using the Vero gimbaled linac system: implementation and first review, *Radiother. Oncol.* 112 (3) (2014) 343–351.

[17] J.W. Wong, M.B. Sharpe, D.A. Jaffray, et al., The use of active breathing control (ABC) to reduce margin for breathing motion, *Int. J. Radiat. Oncol. Biol. Phys.* 44 (4) (1999) 911–919.

[18] V.M. Remouchamps, N. Letts, F.A. Vicini, et al., Initial clinical experience with moderate deep-inspiration breath hold using an active breathing control device in the treatment of patients with left-sided breast cancer using external beam radiation therapy, *Int. J. Radiat. Oncol. Biol. Phys.* 56 (3) (2003) 704–715.

[19] J. Dhont, J. Vandemeulebroucke, M. Burghelée, et al., The long- and short-term variability of breathing induced tumor motion in lung and liver over the course of a radiotherapy treatment, *Radiother. Oncol.* 126 (2) (2018) 339–346.